On the encoding capacity of human motor adaptation

Kim, Seungyeon; Kwon, Jaewoon; Kim, Jin-Min; Park, Frank Chongwoo; Yeo, Sang-Hoon

DOI:
10.1152/jn.00593.2020

Document Version
Publisher's PDF, also known as Version of record

Citation for published version (Harvard):
Kim, S, Kwon, J, Kim, J-M, Park, FC & Yeo, S-H 2021, 'On the encoding capacity of human motor adaptation', *Journal of Neurophysiology*, vol. 126, no. 1, pp. 123-139. https://doi.org/10.1152/jn.00593.2020

american physiological society

JNP JOURNAL OF NEUROPHYSIOLOGY

J Neurophysiol 126: 123–139, 2021.
First published June 2, 2021; doi:10.1152/jn.00593.2020

RESEARCH ARTICLE

Control of Movement

On the encoding capacity of human motor adaptation

Seungyeon Kim,[1] Jaewoon Kwon,[1] Jin-Min Kim,[2] Frank Chongwoo Park,[1] and Sang-Hoon Yeo[2]

[1]*Robotics Laboratory, Department of Mechanical and Aerospace Engineering, Seoul National University, Seoul, South Korea and* [2]*School of Sport, Exercise and Rehabilitation Sciences, University of Birmingham, Birmingham, United Kingdom*

Abstract

Primitive-based models of motor learning suggest that adaptation occurs by tuning the responses of motor primitives. Based on this idea, we consider motor learning as an information encoding procedure, that is, a procedure of encoding a motor skill into primitives. The capacity of encoding is determined by the number of recruited primitives, which depends on how many primitives are "visited" by the movement, and this leads to a rather counterintuitive prediction that faster movement, where a larger number of motor primitives are involved, allows learning more complicated motor skills. Here, we provide a set of experimental results that support this hypothesis. First, we show that learning occurs only with movement, that is, only with nonzero encoding capacity. When participants were asked to counteract a rotating force applied to a robotic handle, they were unable to do so when maintaining a static posture but were able to adapt when making small circular movements. Our second experiment further investigated how adaptation is affected by movement speed. When adapting to a simple (low-information-content) force field, fast (high-capacity) movement did not have an advantage over slow (low-capacity) movement. However, for a complex (high-information-content) force field, the fast movement showed a significant advantage over slow movement. Our final experiment confirmed that the observed benefit of high-speed movement is only weakly affected by mechanical factors. Taken together, our results suggest that the encoding capacity is a genuine limiting factor of human motor adaptation.

NEW & NOTEWORTHY We propose a novel concept called "encoding capacity" of motor adaptation, which describes an inherent limiting-factor of our brain's ability to learn new motor skills, just like any other storage system. By reinterpreting the existing primitive-based models of motor learning, we hypothesize that the encoding capacity is determined by the size of the movement, and present a set of experimental evidence suggesting that such limiting effect of encoding capacity does exist in human motor adaptation.

encoding capacity; motor adaptation; motor primitives; signal-dependent noise

INTRODUCTION

Existing models of human motor control tend to depreciate the value of making larger movements when learning motor skills. A well-known fact about human movement is that larger movements are accompanied by higher control noise (1) and more complex inertial force (2), not to mention higher metabolic costs (3). Because of those clear drawbacks, making larger movements does not seem to have any point or purpose. However, here we claim that larger and more dynamic movements bring substantial benefits in motor adaptation, especially when learning the complex dynamics of the body and external environments. We propose that this benefit comes from a previously unstudied factor that a larger movement increases the "capacity" of adaptation, allowing more complicated dynamics information to be "encoded" in the internal model.

The predominant theory of human motor adaptation proposes that the dynamics of learned motor tasks is represented as state-dependent policies, specifying what action needs to be taken for a given state of the sensorimotor system (4–6). Specifically, these policies are internally modeled as population responses of motor primitives distributed in the state-space, where each primitive contains localized information of the policy and its generalization pattern to neighboring states (7, 8). The precise form of the motor primitives, that is, in what domain the state-space is defined, how their receptive fields are shaped, or what are their outputs,

Correspondence: S.-H. Yeo (s.yeo@bham.ac.uk).
Submitted 12 October 2020 / Revised 7 May 2021 / Accepted 26 May 2021

are still ongoing research topics in motor control (7, 9–15). However, in any case, all primitive-based internal models intrinsically possess limitations in their expressiveness: perfectly learnable force fields are confined to a subspace that can be expressed by a set of primitives recruited for learning; otherwise, the internal model only can learn the force field approximately, even if the number of learning trials is sufficient for the adaptation. Despite the lack of thorough investigation, the existence of such an intrinsic ceiling, that is, the capacity of motor adaptation imposed by the primitive-based adaptation mechanism, has been observed in the previous studies (7, 16, 17).

Focusing on this aspect, we consider motor learning as an information encoding procedure; that is, a procedure for encoding a certain motor skill into internal storage, that is, a group of motor primitives in the state-space. The amount of information to encode corresponds to the complexity of the motor skill, and the "motor encoding capacity," the maximum amount of information that can be held by the internal model, is determined by the number of primitives that are engaged in the encoding procedure. Importantly, the gradient-decent-type learning rule that the brain is likely to incorporate (7, 16) imposes that only motor primitives adjacent to the movement trajectory are recruited for adaptation, and therefore the encoding capacity of a motor skill is determined and limited by the movement itself.

In this study, we focus on how the encoding capacity limits its learning to make circle-drawing movements against an angle-dependent, radially perturbing force field. We predict that, when the radius of the circle is fixed, faster movement has higher encoding capacity, as fast movements form larger circles in the velocity space and therefore can recruit more motor primitives, allowing a larger amount of information to be encoded. If we assume that the amount of information is related to the complexity of the radial force field, this leads to a testable hypothesis that we can adapt to a more complex radial force field when we are making higher-speed circular movements.

This hypothesized effect of encoding capacity can be conceptually demonstrated by a simple computational simulation. To our circle-drawing scenario, we applied the classic motor adaptation model by Thoroughman and Shadmehr (7), where motor primitives are represented as Gaussian-like receptive fields laid out in the velocity space and the activation levels of the primitives are updated every cycle of the circle drawing based on the gradient of the force error. Same as our human experiment, which will be introduced later (*experiment 2*, see MATERIALS AND METHODS), we tested how well the computational model learns simple and complex force fields under fast and slow circular movements. The result of the simulation, summarized in Fig. 1, supports our hypothesis. As expected, a faster circular movement, represented as a larger circle in the velocity space, can recruit a

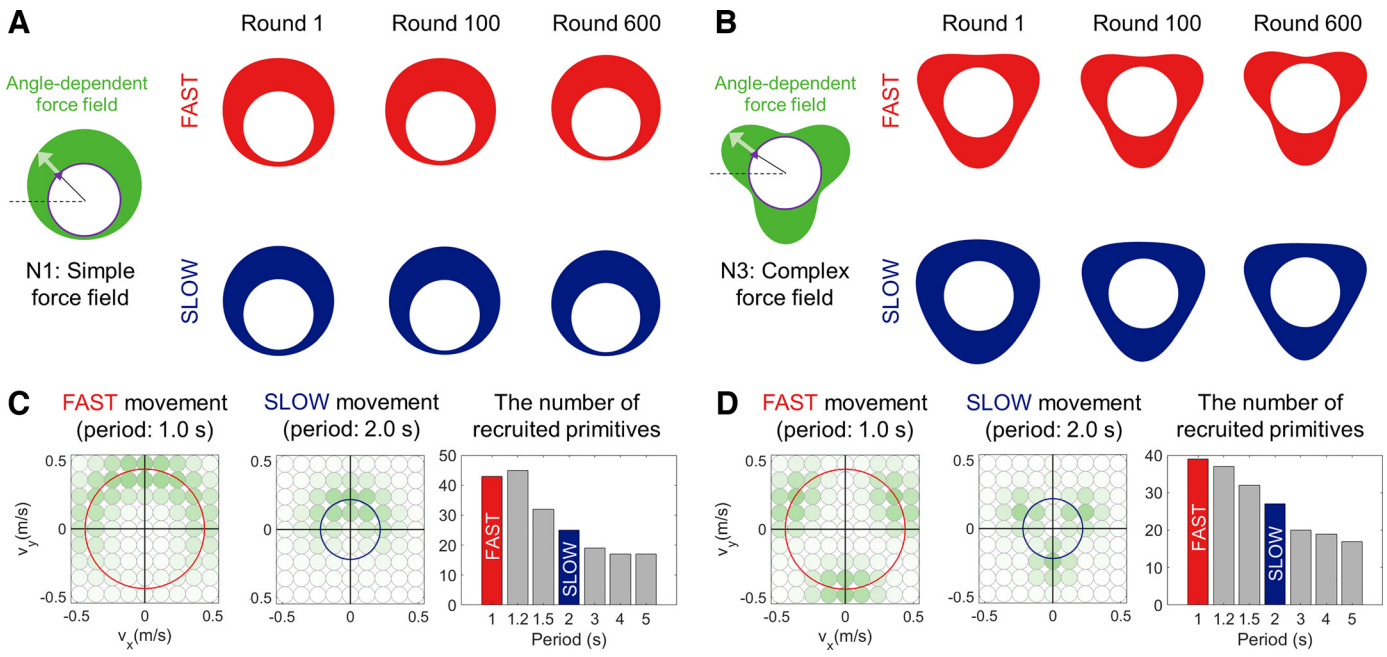

Figure 1. Conceptual simulation of the limiting effect of encoding capacity in motor adaptation. *A* and *B*: simulations of adaptation to force fields used in our human experiment (*experiment 2*). A primitive-based motor adaptation model by Thoroughman and Shadmehr (7) was applied to adjust responses of motor primitives for each cycle of circle drawing to compensate for an angle-dependent radial force field. A total of 600 cycles, similar to the number of cycles used in our human experiment, was used for adaptation. Same as *experiment 2*, the simulation used two different types of force field, i.e., simple (N1 force field, indicated as a green envelope on the left; *A*) and complex (N3 force field; *B*) under two different speed conditions, named FAST and SLOW. See MATERIALS AND METHODS for details of this experimental design. Circles with red (FAST) and blue (SLOW) envelopes show the encoded force field in different phases of adaptation. *C* and *D*: the left and center plots visualize the activation of motor primitives at the end of adaptation (i.e., at cycle 600), drawn in the two-dimensional velocity space. Same as Thoroughman and Shadmehr (7), primitives were modeled as Gaussians with standard deviation σ = 0.12 m/s, and the distance between neighboring primitives was set to σ. Reference trajectories for FAST and SLOW conditions are drawn as red and blue circles, respectively. Activation levels of primitives are indicated by green color with varying intensities. Bar plots on the right show the simulated number of recruited primitives for different periods of circle drawing including those for FAST and SLOW conditions.

J Neurophysiol • doi:10.1152/jn.00593.2020 • www.jn.org

greater number of primitives (Fig. 1, *C* and *D*). This increased encoding capacity of faster circle drawing does not have a noticeable effect when learning a simple force field (Fig. 1*A*) that is sufficiently learnable for both speed conditions. However, when learning a complex-shaped force field (Fig. 1*B*), the simulation predicts a clear benefit of fast movement. With slow movements, the force field can only be partially learned despite extended training (600 cycles) because of the limited encoding capacity. Therefore, prediction from the conventional model conceptually legitimizes our experimental hypothesis.

Despite this logical possibility, very little prior research in motor learning has investigated the existence of such benefits of higher speed movements. Furthermore, this view sharply contradicts the conventional perspective on the adverse effect of the speed on motor performance caused by the increased uncertainty because of signal-dependent noise (1, 18), which is considered to impede the adaptation (19). Therefore, we expect to see an interaction between the effect of motor encoding capacity and that of the signal-dependent noise, forming a trade-off between high-precision, low-capacity (slower the better) and low-precision, high-capacity (faster the better) movement. The primary goal of this study is therefore to experimentally demonstrate the existence of the motor encoding capacity as one of the critical limiting factors of human motor adaptation and to explore how its effect is behaviorally manifested through interaction with other movement factors.

MATERIALS AND METHODS

Ethics Statement

The University of Birmingham Ethics Board approved the study, and the participants gave written informed consent before participating.

General Description

The study consisted of three experiments, referred to as *experiment 1*, *experiment 2*, and *experiment 3* hereafter. *Experiment 1* tested whether learning requires movement, that is, a nonzero encoding capacity, by testing participants' ability to learn a predictable rotating force under two conditions: *1*) when maintaining a static posture and *2*) when making a small movement in synchrony with the rotating force. In *experiment 2*, we further investigated the effect of encoding capacity on the adaptation performance. Based on the assumption that the encoding capacity is modulated by the speed of movement, we tested whether higher speed movement facilitates learning a more complex force field. Finally, in *experiment 3*, we verify whether such benefit of high-speed movement mainly originates from the state-dependent primitive mechanism.

A total of 30 naive human participants (aged 25.1 ± 2.5 yr, 12 females) participated in the three experiments (6 participants for *experiment 1*, 16 for *experiment 2*, and 8 for *experiment 3*). All participants were right-handed according to the Edinburgh handedness inventory (20) and had no reported neurological disorders. The participants were seated and grasped the handle of a vBOT planar robotic manipulandum (21) with their dominant hand. A mirror reflecting a top-mounted computer screen was located between participants' eyes and their hands, and provided vertical visual feedback of their hand position as a yellow filled cursor of a 0.5-cm radius. The height of the seat was adjusted so that the upper arm was held parallel to the ground and the right knee was just below the reference point (or the center of the reference circle) to provide a comfortable configuration for performing the tasks. After a brief familiarization period, participants were asked to maintain static posture or to make circular movements along a reference circle displayed on the screen in a constant frequency, indicated by a tone or by a target cursor movement. While performing the task, the robot applied force perturbations generated by different force fields specified in each experiment, and participants were instructed to cope with the perturbing forces to minimize the deviation of the cursor from the reference point or circle while maintaining the required rotation frequency. In addition to those force-fields, a mild damping force with a damping ratio 0.04 Ns/cm was added by default to maintain the overall stability of the handle.

Experiment 1

Experiment 1 was focused on evaluating the adaptation performance to a "time-dependent periodic force," defined as:

$$\begin{bmatrix} F_x \\ F_y \end{bmatrix} = (a + b\sin 4\pi t)\begin{bmatrix} -\cos 4\pi t \\ \sin 4\pi t \end{bmatrix}(\mathrm{N}), \qquad (1)$$

where a and b are set to 4.4 N and 3.52 N, respectively. Participants were instructed to compensate this force field under two different task conditions: *1*) HOLD: participants were instructed to try maintaining the cursor completely static, that is, without compromisingly making any oscillatory movements, on the reference point against perturbing forces; and *2*) DRAW: participants were asked to draw a small circle of radius 2 cm with the same frequency, that is, 2 Hz, to the rotating force. Graphical descriptions of the two conditions can be found in Fig. 2*A*. The performance of adaptation was measured by taking the average error around the reference trajectories, that is, a point for HOLD and a circle for DRAW. Participants conducted both conditions within a single visit where the order of conditions was counterbalanced across the participants.

The experiment consisted of 35 blocks and each block lasted for 5 s, which allowed the 2 Hz time-dependent periodic force to rotate 10 times per each block. In the HOLD condition, the participants performed the task of maintaining static posture on the reference point (displayed as a filled white circle with radius 0.5 cm). The first five blocks were the preexposure phase (blocks 1–5), applying the null force field to the participants (i.e., only the mild damping force was applied). Then, the exposure phase with the time-dependent force field was started (blocks 6–35). The block composition is the same with the DRAW condition, and the overall block composition can be found in Fig. 2*B*. The tick-tock sound was played with the same frequency to the time-dependent periodic force to help participants maintain their tempo. Participants took a 30 s mandatory break for every 10 blocks but were also encouraged to take rests in-between blocks if they wished to. The error was defined as the distance between the reference point and the cursor. The average

error was calculated using classical root mean square error for every 5 s, and error feedback was provided in real-time during the movement based on the average error. The feedback message for average error less than 2 cm was "great," for 2–3 cm was "good," and for average error greater than 3 cm was "try harder." In the DRAW condition, the participants performed the task of drawing a small reference circle (displayed as a dark green ring with a radius of 2 cm and a thickness of 0.5 cm) with the same frequency as the time-dependent periodic force. The participants were instructed to keep the trajectory of their hands as circular as possible. The rest of the design was identical to the HOLD condition, except that the error was defined as the shortest distance from cursor to the reference circle.

Experiment 2

Experiment 2 used the "state-dependent force field," defined as:

$$\begin{bmatrix} F_x \\ F_y \end{bmatrix} = (a + b \sin n\theta) \begin{bmatrix} \cos\theta \\ \sin\theta \end{bmatrix} (\mathrm{N}), \qquad (2)$$

where a and b have same values to the time-dependent force field used in *experiment 1*, and $\theta = \arctan 2(y, x)$ is the angle between the horizontal axis (x-axis) and the vector from the origin to the handle. Note that the time-dependent periodic force and the state-dependent force field are phenomenologically identical if the participants make a perfectly circular movement with a constant angular velocity. The complexity of a state-dependent force field was adjusted by the complexity index n, indicating the frequency of how many times the force oscillates from maximum to minimum per one cycle. In our study, to represent simple and complex dynamics to adapt, state-dependent force fields with complexity indices 1 (simple) and 3 (complex) were used, and they were named as "N1" and "N3" force field, respectively. The shapes of these force fields are illustrated in Fig. 3*A* and Fig. 4*A*, respectively.

A total of 16 participants were divided into two groups of eight each, and performed circle-drawing tasks while adapting to the following different types of radial force fields: one group was given the N1 force field and another group was given the N3 force field. Both the N1 and N3 groups performed circle-drawing tasks of radius 7 cm under two different speed conditions: *1*) FAST: one cycle per second and *2*) SLOW: one cycle per 2 s. Therefore, there were a total of four different experimental conditions across two participant groups: N1-FAST and N1-SLOW for the N1 group, and N3-FAST and N3-SLOW for the N3 group. The experiment in each condition consisted of seven preexposure blocks followed by 40 exposure and 3 postexposure blocks (Fig. 3*B* and Fig. 4*B*), where each block consisted of 12 continuous rotations. In addition, some blocks contain error clamp trials (see *Error Clamp Trials* for detail) to analyze the active force compensation, and we measured the electromyogram (EMG) of four representative upper-limb muscles (biceps, triceps, pectoralis, and deltoid) for the N3 group (i.e., N3-SLOW and N3-FAST conditions) to check the level of muscle cocontractions (see *EMG Analysis* for further details).

To avoid the order effect, half (i.e., 4) of the participants in each group performed the FAST condition first and the other performed the SLOW condition first. In addition, to prevent the transfer of learning across two consecutive sessions, one of two sessions used a horizontally flipped force field (Fig. 3*A* and Fig. 4*A*). Participants were instructed to keep the trajectories of their hands as close to the reference circle as possible. To assist participants to keep their desired tempos, tick-tock sounds were played in the desired frequency. In addition, visual pacemakers were displayed to provide additional guidance on the desired movement frequency: pacemakers were displayed as two radially aligned line segments in red, placed on the reference circle, spaced 180° apart, and rotating in the desired frequency. This was based on the previous study on circular movements by Howard et al. (22), in which a similar type of pacemakers was used to encourage participants to maintain their tempo around the desired frequency, but without triggering any feedback tracking behavior. As in Howard et al.'s study, participants were instructed not to follow these cursors, but only to use them as pacemakers. Last, an afterimage of the cursor was also displayed during the movement, visualizing the recent trajectory of the cursor for the last 3 s as a thin green curve of width 0.2 cm. This helped participants to self-assess their circle-drawing performance in real-time.

Each speed condition consisted of 50 blocks for each speed condition, each of which was divided into three phases: preexposure phase (blocks 1–7), exposure phase (blocks 8–47), and postexposure phase (blocks 48–50). There were two types of blocks; null and probe. Each null block consisted of 12 normal rotations, and each probe block contained one error clamp trial (2 rotations) inserted between the 5th and the 9th of 10 normal rotations in a randomized way. The preexposure phase consisted of four null blocks (blocks 1–4) and three probe blocks (blocks 5–7). All blocks in the exposure and the postexposure phase except the early-exposure phase (blocks 8–9) were probe blocks. The reason why probe block was not used in early preexposure and exposure phase is to avoid excessive confusions of the participants: through preliminary experiment, it has been found that making participants experience error clamp trials from the very beginning of the preexposure and exposure phase, that is, while they are familiarizing themselves to the experimental environment and also to the imposed force fields, tends to cause a great deal of confusion, despite considerations to minimize disruption by error clamp trials in a circular mechanical channel (see *Error Clamp Trials* below for details).

Participants took a 30 s mandatory break for every 10 blocks, resulting in five mandatory breaks in total for each condition, but were also encouraged to take a rest between blocks if they wish to. The error, the average error, and the corresponding feedback were defined and displayed in the same way as with the DRAW condition in *experiment 1*, except that the average error was calculated for each rotation, that no error feedback was provided during the error-clamp trials, and that the feedback for average error less than 0.6 cm was "great," for 0.6–0.8 cm was "good," and for average error >0.8 cm was "try harder." For data in the error clamp trials, the average force trajectory of the preexposure phase (blocks 5–7) was taken as the baseline and subtracted from the force trajectory of other blocks for each participant.

Experiment 3

To check the potential mechanical effect, referred to as "instantaneous stabilization" later in RESULT, on the performance of circle drawing in *experiment 2*, *experiment 3* was focused on quantifying how much the performance of fast movement under the N3 force field, that is, performance under N3-FAST condition, is affected if the state-dependency of the task is selectively muted; This was done by slightly desynchronizing the state-force relationship of the N3 force field. We call this new force field the "asynchronous N3" (N3a) force field. The N3a force field was defined as:

$$\begin{bmatrix} F_x \\ F_y \end{bmatrix} = (a + b\sin n\frac{2\pi - 0.3}{2\pi}(\theta - \theta_0))\begin{bmatrix} \cos\theta \\ \sin\theta \end{bmatrix}(\mathrm{N}), \quad (3)$$

where a and b have the same values, and in this case, θ is the cumulative angle that does not reset to 0 when it exceeds 2π and keeps increasing. In the other words, the term $\theta - \theta_0$ means the moving angle which starts from 0 in the initial position. As shown in the equation, the scalar term 0.3 causes a slight desynchronization and therefore breaks the state-dependency, which means that when circle is being drawn, the force field rotates ~17.2° per cycle. Figure 8*A* illustrates the N3 and N3a force field used in *experiment 3*.

Eight naive subjects participated in *experiment 3*. Each participant conducted two experimental sessions, N3 and N3a force field adaptations in the FAST condition of *experiment 2*, within a single visit. The order of the sessions was counterbalanced across the participants. The experimental design of each session was identical to the N3-FAST condition in *experiment 2*, except for the fact that the N3a force field was used in the N3a session (Fig. 8*B*).

Incremental Area under the Curve

As the measure of adaptation performance, we used the area under the curve (AUC), that is, the total error, as used in previous studies (23). However, since the baseline levels for the FAST and SLOW conditions in *experiment 2* are substantially different, we adopted the baseline-adjusted metric, incremental area under the curve (iAUC). As the name stands, iAUC is the integral of the learning curve minus the area below the baseline. For each adaptation curve in *experiment 2* and *experiment 3*, the baseline was determined per subject by the mean error level during the preexposure phase and the area under the curve was computed via the trapezoidal method.

Error Clamp Trials

Trials in *experiment 2* and *experiment 3* included error clamp trial. In contrast to the conventional error clamp trials implemented as a rigid mechanical channel for point-to-point movement (24), a circular version of error clamp trial was used, during which the hand was constrained in a circular mechanical channel and the force applied against the channel was measured. Along the reference circle of a 7 cm radius, a stiff mechanical channel with a width of 0.01 cm was generated during the error clamp trial. The mathematical definition is:

$$\begin{bmatrix} F_{Cx} \\ F_{Cy} \end{bmatrix} = -K\begin{bmatrix} g(x,y) \\ h(x,y) \end{bmatrix}(\mathrm{N})$$

$$g(x,y) = \begin{cases} x - (R-d)\cos\theta & x^2 + y^2 \le (R-d)^2 \\ 0 & (R-d)^2 < x^2 + y^2 \le (R+d)^2 \\ x - (R+d)\cos\theta & x^2 + y^2 > (R+d)^2 \end{cases}(\mathrm{cm})$$

$$h(x,y) = \begin{cases} y - (R-d)\sin\theta & x^2 + y^2 \le (R-d)^2 \\ 0 & (R-d)^2 < x^2 + y^2 \le (R+d)^2 \\ y - (R+d)\sin\theta & x^2 + y^2 > (R+d)^2 \end{cases}(\mathrm{cm}), \quad (4)$$

where d = 0.005 cm and R = 7 cm. The value of spring stiffness was set as K = 80 N/cm. As one block in our experiment consisted of continuous circular movements, our error clamp trial was implemented in such a way that one of the turns was randomly picked and switched to the error clamp trial. Because of this continuity, directly introducing the mechanical channel was impracticable as it often caused excessive mechanical impacts. Therefore, the beginning and the end of the error clamp trial were padded with smooth fade-in and fade-out half-turns, during which the mechanical channel smoothly appeared or disappeared. This made the error clamp trial to consist of two full turns. If φ be the angle of the handle in the error clamp trial (i.e., $\varphi \in [0,4\pi]$), we defined an α function $\alpha(\varphi)$ expressed as:

$$\alpha(\varphi) = \begin{cases} \varphi/\pi & 0 \le \varphi < \pi \\ 1 & \pi \le \varphi < 3\pi \\ 4 - \varphi/\pi & 3\pi \le \varphi \le 4\pi \end{cases}. \quad (5)$$

If the force applied during normal trials is $[F_{Dx}\ F_{Dy}]^T$, then the participant receives the force during the error clamp trial:

$$\begin{bmatrix} F_x \\ F_y \end{bmatrix} = (1 - \alpha(\varphi))\begin{bmatrix} F_{Dx} \\ F_{Dy} \end{bmatrix} + \alpha(\varphi)\begin{bmatrix} F_{Cx} \\ F_{Cy} \end{bmatrix}(\mathrm{N}). \quad (6)$$

Using this α function, the mechanical channel was linearly engaged and disengaged during the first and last half turns respectively, without abruptly interrupting the present force field in normal trials. For error clamp trials, we compute the force compensation rate by linear regression of the measured force pattern onto the desired force pattern, as used in previous studies (25, 26). The slope obtained as a result of linear regression is defined as the force compensation rate. This force compensation rate is zero when the force trajectories are uncorrelated and one if the measured force trajectory is identical to the desired force trajectory.

EMG Analysis

For the N3 group of *experiment 2*, surface EMGs of four major muscles of the upper limb, pectoralis major, posterior deltoid, triceps long head, and biceps long head, were measured using a single differential electrode EMG system (Delsys Bagnoli DE-2.1). Electrodes were placed over the muscle bellies and the analog signals were transferred to a desktop PC using a multifunction in/out device (NI PCIe-6323). The measured EMG signals were observed in real-time via MATLAB Simulink (2019 b) and simultaneously stored in the PC. Collected

EMG signals were low-pass filtered in MATLAB (Butterworth 4th order, 10 Hz cut-off frequency) and were averaged over each block. To handle between-subject variability of the EMG levels, EMG data per participant was normalized with respect to the average EMG level in the SLOW condition of the late pre-exposure phase (blocks 5–7) of each subject. Six participants' data in the N3 group were measured, but still maintained counterbalanced to speeds. Pectoralis data of one participant were excluded in the analysis since the participant had a mild skin irritation issue, resulting in a highly atypical EMG pattern.

Statistical Analysis

Data were analyzed using MATLAB R2018a and statistical tests were performed using SPSS Statistics 25. Statistical significance was considered at the $P < 0.05$ level for all tests. In the figures, n.s. indicates no significance, * indicates $P < 0.05$, ** indicates $P < 0.01$, and *** indicates $P < 0.001$.

Data Availability

The data that support the findings of this study are available from the corresponding author upon request.

RESULTS

Experiment 1: Learning a Motor Skill Necessitates Movements

The result of *experiment 1* is summarized in Fig. 2. During the preexposure phase, participants stayed static in HOLD and made circular movements in DRAW as instructed (Fig. 2*C*, preexposure). As expected, the error level of DRAW during the preexposure phase was significantly higher than that of HOLD (Fig. 2*D*, blocks 1–5; $F_{1,5} = 17.774$; $P = 0.008$). When the time-dependent periodic force was introduced, the hand paths in both conditions deviated substantially from their references (Fig. 2*C*, early-exposure), indicated by significantly high error levels in the early-exposure phase (Fig. 2*D*, blocks 4–8; $F_{4,20} = 44.377$; $P < 0.001$ for HOLD and $F_{4,20} = 15.798$; $P < 0.001$ for DRAW). As exposure to this force field continued, participants were able to reduce the error substantially in DRAW (Fig. 2*D*, blocks 6–7 and 33–35, light blue; $F_{4,20} = 6.115$; $P = 0.002$), down to a similar level to the baseline (Fig. 2*C*, late-exposure, light blue). However, participants were unable to reduce the error in HOLD (Fig. 2*D*, blocks 6–7 and 33–35, orange; $F_{4,20} = 0.888$; $P = 0.489$) and therefore the error remained high, or even became higher, during the entire exposure phase (Fig. 2*C*, late-exposure,

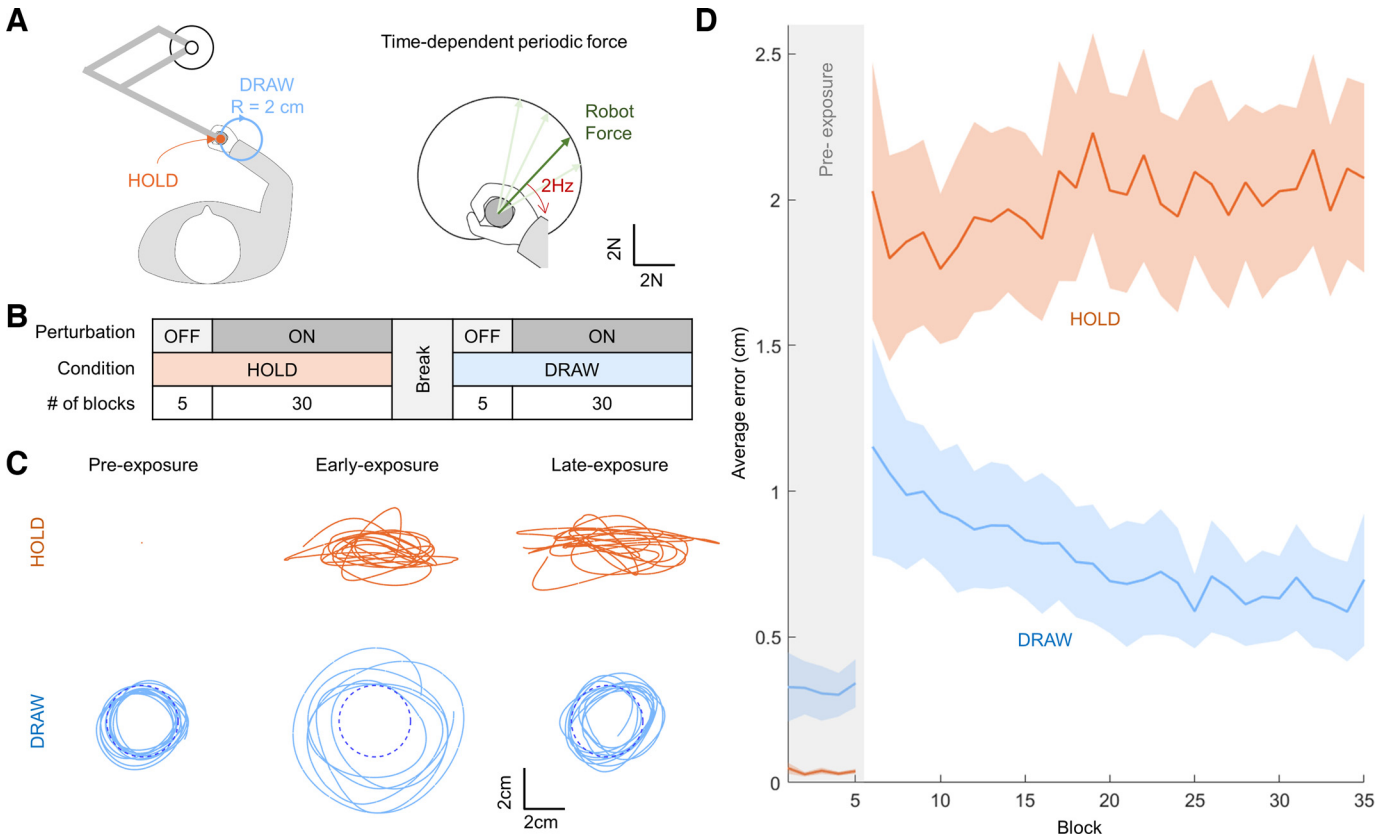

Figure 2. *Experiment 1*: learning a motor skill necessitates movements. *A*: experimental setup: participants held the handle of the robotic manipulandum and performed two tasks (*left*): HOLD (orange dot) and DRAW (light blue circle). While performing the tasks, the robot applied a time-dependent periodic force to the handle (*right*). *B*: experimental protocol. *C*: representative hand paths of HOLD (orange) and DRAW (light blue) during preexposure (block 5), early-exposure (block 6), and late-exposure (block 35) phases. The reference circle for DRAW is drawn as a broken circle. *D*: adaptation curves of HOLD (orange) and DRAW (light blue), shown as block number vs. corresponding means ± standard error across all six participants ($n = 6$). One-way repeated-measure ANOVA was used for statistical tests on average errors.

J Neurophysiol • doi:10.1152/jn.00593.2020 • www.jn.org

orange). This suggests that participants were able to compensate for the periodic force pattern in the DRAW task but not in the HOLD task.

The HOLD task can be considered as a classical adaptive control problem, where a controller is required to learn the periodic external forces and develop a counteracting control strategy generating time-dependent (i.e., periodic) control forces. The result suggests that participants were unable to develop such a time-dependent strategy, which reconfirms the result of a previous study on the lack of time-dependency in motor adaptation (27). This would have been the same for the DRAW task, but it is likely that participants have developed a state-dependent strategy equivalent to the time-dependent strategy since the periodic force can be regarded as an angle-dependent (i.e., state-dependent) force field when the frequency of the circle-drawing is synchronized to that of the perturbing forces (27–29), building a one-to-one relationship between the state of the hand position and the phase of the force. Since the only difference between the two tasks was that DRAW involves movement whereas HOLD does not, the result suggests that movement is an important factor that enables adaptation. From the perspective of the encoding capacity, this can be restated as that adaptation requires nonzero encoding capacity, that is, a group of motor primitives being involved.

Experiment 2 with N1 Group: When Learning a Simple Force Field, Higher Speed Has No Benefit on the Adaptation Performance

In *experiment 2*, we further explored how the encoding capacity, determined by the size of the movement, limits the adaptation performance, and how it interacts with the complexity of the force field to learn. Figure 3 summarizes the experimental result of the N1 group (N1-SLOW and N1-FAST). In the preexposure phase, participants successfully made circular movements at both speeds, with higher variability in N1-FAST (Fig. 3*C*, preexposure), and accordingly, a significantly higher average baseline error observed in the N1-FAST as expected (Fig. 3*D*, blocks 5–7; $F_{1,7} = 14.500$; $P = 0.007$). When the N1 force field was introduced, hand trajectories in both conditions became significantly deviated outwardly from the circular shape because of radially perturbing forces (Fig. 3*C*, early-exposure; Fig. 3*D*, blocks 6–10; $F_{4,28} = 29.847$; $P < 0.001$ for FAST and $F_{4,28} = 25.505$; $P < 0.001$ for SLOW), but participants were able to significantly reduce the error in the later exposure blocks for both speed conditions (Fig. 3*C*, late-exposure; Fig. 3*D*, blocks 9–10 and 45–47; $F_{4,28} = 4.800$; $P = 0.004$ for FAST and $F_{4,28} = 18.274$; $P < 0.001$ for SLOW). Notably, the significant difference between the errors in the two conditions persisted in the late-exposure phase (Fig. 3*D*, blocks 45–47; $F_{1,7} = 18.748$; $P =$

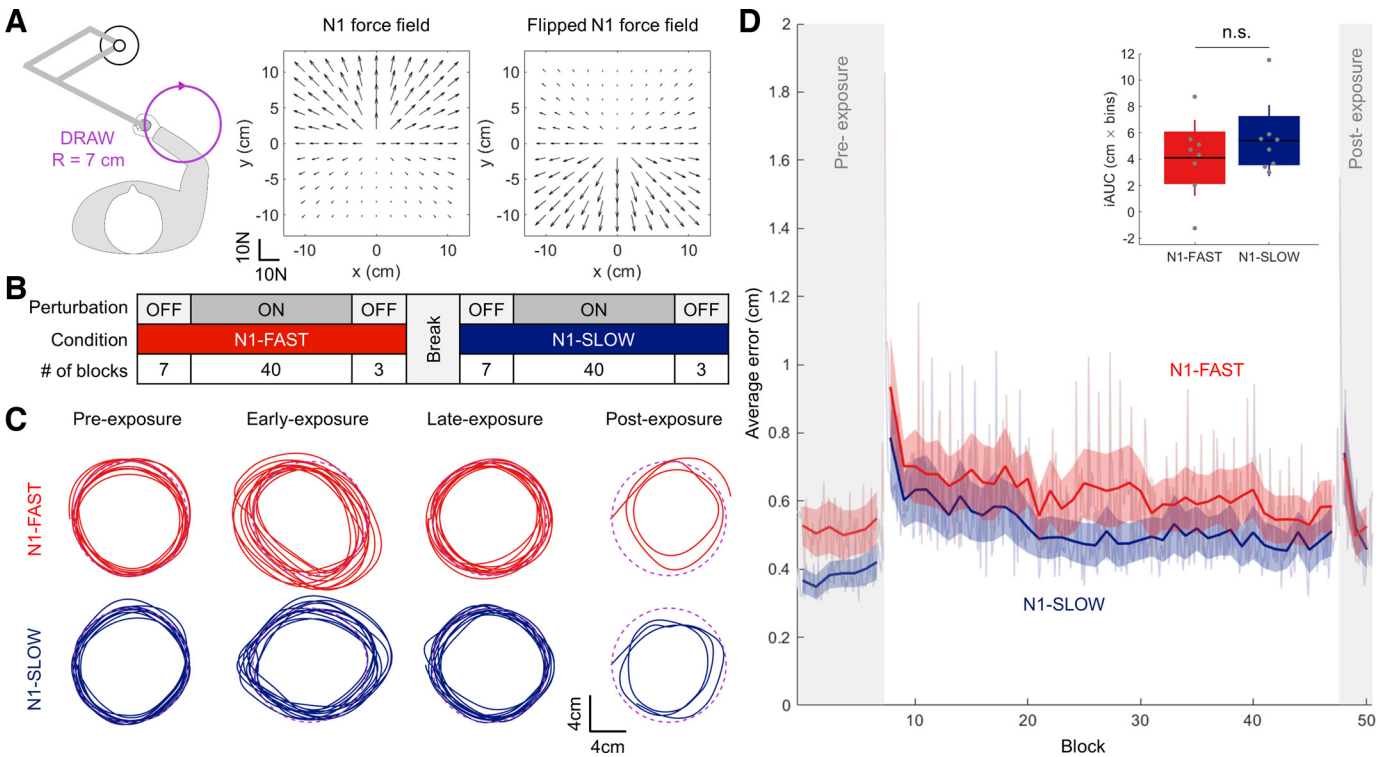

Figure 3. *Experiment 2* with N1 group: when learning a simple force field, higher speed has no benefit on the adaptation performance. *A*: experimental setup: participants performed clockwise circle-drawing tasks under the N1 force field (*left*). The N1 force field and its flipped version are shown as vector fields in the positional space (*center* and *right*). *B*: experimental protocol. *C*: representative hand paths of N1-FAST (red) and N1-SLOW (blue) during preexposure (block 7), early-exposure (block 8), late-exposure (block 47), and postexposure (block 48) phases. Reference circles are drawn as broken circles. *D*: adaptation curves of N1-FAST (red) and N1-SLOW (blue), shown as block number vs. corresponding means ± standard error across all eight participants ($n = 8$). The pale-colored graph in the background shows the magnitude of the errors on a per-cycle basis. One-way repeated-measure ANOVA was used for statistical tests on average errors. *Inset* is a box plot of incremental area under the curve (iAUC) values for each speed condition. A paired *t* test was used for statistical tests on iAUC values.

0.003). When the force field was turned off, the trajectories in both conditions were again significantly deviated from the reference circle but inwardly (Fig. 3*C*, Postexposure) by which the error level became higher again (Fig. 3*D*, blocks 46–48; $F_{2,14} = 6.031$; $P = 0.013$ for FAST and $F_{2,14} = 8.448$; $P = 0.004$ for SLOW), suggesting that there were aftereffect. Error levels in the post-exposure phase compared to the late-exposure phase were not significantly different across two speed conditions (Fig. 3*D*, block 48; $F_{1,7} = 3.874$; $P = 0.090$).

To avoid confusion, we use the term "motor performance," the net performance of circle drawing, separately from the "adaptation performance." Comparing the adaptation curves of two conditions, it is clear that the motor performance in N1-FAST was consistently worse because of the inherent signal-dependency of motor noises, which is already noticeable in the baseline level. We analyzed whether this higher error level has affected the adaptation performance during the exposure phase using a baseline-adjusted statistical test, iAUC with respect to the average preexposure (i.e., the baseline) error (see *Incremental Area under the Curve* in MATERIALS AND METHODS). A paired t test on iAUC values of the exposure phase revealed that there is no significant difference in iAUC values between N1-FAST and N1-SLOW (Fig. 3*D*; $t_7 = -1.326$; $P = 0.227$), suggesting that the higher error level of N1-FAST did not have a significant impact on the adaptation performance. Looking at the aftereffect in the early post-exposure phase, the relative increases of the error level with respect to the late-exposure phase for two speed conditions were not significantly different. Altogether, these results suggest that the adaptation performance of N1-FAST was no better than that of N1-SLOW.

Experiment 2 with N3 group: When Learning a Complex Force Field, Higher Speed Improves the Adaptation Performance

Figure 4 summarizes the experimental result of the N3 group (N3-SLOW and N3-FAST). Because of the increased complexity of the force field, trajectories during the early phase of the adaptation show greater and more complicated deviations from the reference circle (Fig. 4*C*, early-exposure; Fig. 4*D*, blocks 6–10; $F_{4,28} = 34.043$; $P < 0.001$ for FAST and $F_{4,28} = 46.958$; $P < 0.001$ for SLOW), compared to those in the N1 group. These errors were significantly reduced throughout the adaptation trials in both conditions (Fig. 4*D*, blocks 9–10 and 45–47; $F_{4,28} = 27.649$; $P < 0.001$ for FAST and $F_{4,28} = 17.476$; $P < 0.001$ for SLOW), but a faster reduction was observed in N3-FAST, resulting in more circular trajectories (Fig. 4*C*, late-exposure) and significantly lower error level in the late-exposure phase (Fig. 4*D*, blocks 45–47; $F_{1,7} = 22.054$; $P = 0.002$). A paired t test confirmed that the iAUC of the entire exposure phase of N3-SLOW was significantly higher than that of N3-FAST (Fig. 4*D*; $t_7 = -5.432$; $P = 0.001$). This suggests that the learning was facilitated more in N3-FAST,

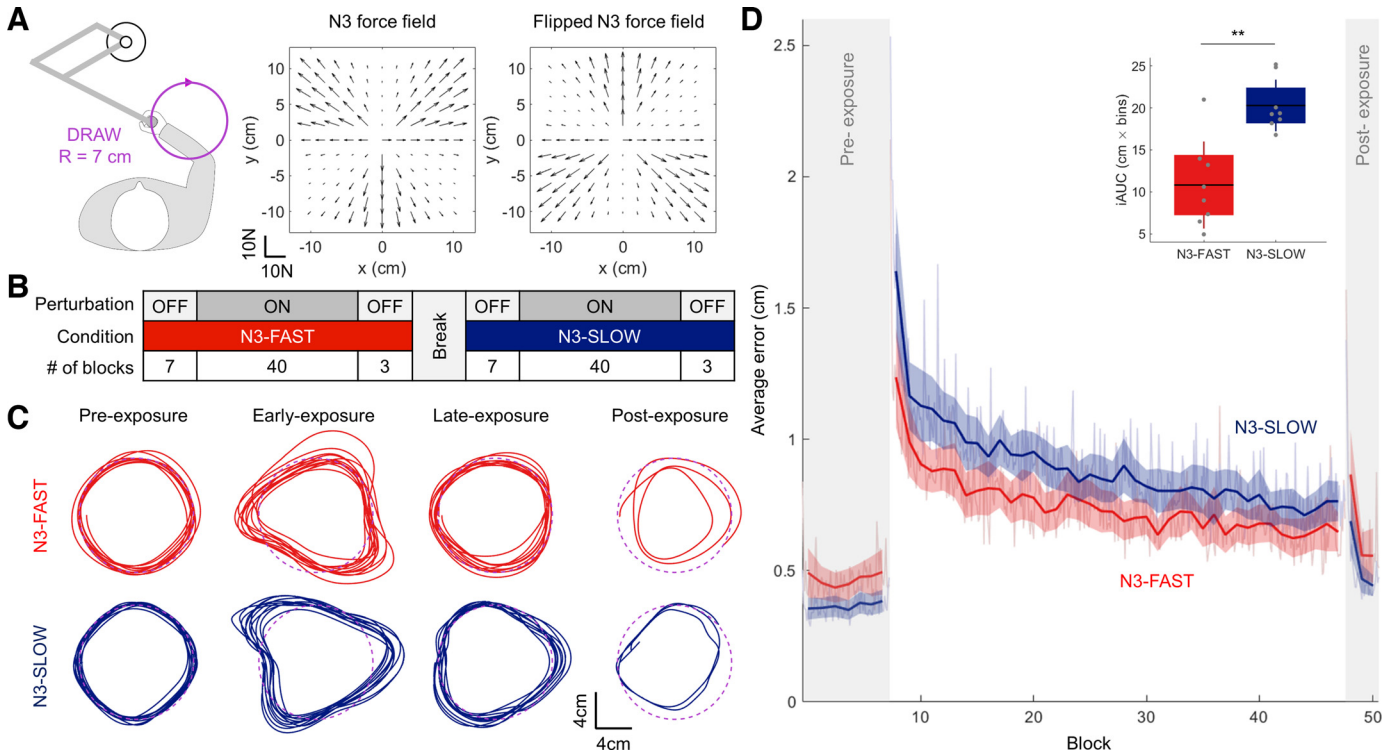

Figure 4. *Experiment 2* with N3 group: when learning a complex force field, higher speed improves the adaptation performance. *A*: experimental setup: participants performed clockwise circle-drawing tasks under the N3 (complex) force field (*left*). The N3 force field and its flipped version are shown as vector fields (*center* and *right*). *B*: experimental protocol. *C*: representative hand paths of N3-FAST (red) and N3-SLOW (blue) during preexposure (block 7), early-exposure (block 8), late-exposure (block 47), and postexposure (block 48) phases. Reference circles are drawn as broken circles. *D*: adaptation curves of N3-FAST (red) and N3-SLOW (blue), shown as block number vs. corresponding means ± standard error of all eight participants ($n = 8$). The pale-colored graph in the background shows the magnitude of the errors on a per-cycle basis. One-way repeated-measure ANOVA was used for statistical tests on average errors. Inset is a box plot of incremental area under the curve (iAUC) values for each speed condition. A paired t test was used for statistical tests on iAUC values.

which contrasts sharply with the result of the N1 group. Similarly, the aftereffect of N3-FAST with respect to the error level in the late-exposure phase was significantly higher than that of N3-SLOW (Fig. 4*D*, Block 48; $F_{1,7} = 6.414$; $P = 0.039$).

Although high-speed movements clearly had a beneficial effect on the adaptation performance, there was an effect of the speed on the motor performance that did not seem to be related to the adaptation. The initial part of adaptation curves suggests that the initial error level of N3-FAST was already significantly lower in the early-exposure (Fig. 4*D*, blocks 8–10; $F_{1,7} = 9.699$; $P = 0.017$), whereas the initial error level of N1-FAST was significantly higher than that of N1-SLOW (Fig. 3*D*, blocks 8–10; $F_{1,7} = 20.496$; $P = 0.003$). This can be also observed in *experiment 1*, where there was an instantaneous drop of the error in DRAW compared with that of HOLD. In addition, faster deadaptation observed in all experiments may also be affected by this instantaneous reduction. These observations indicate that the observed difference in the performance may have been influenced by some neuromechanical factors, such as an increased level of arm impedance because of cocontracting muscles (30, 31) or up-regulated reflex gains (32, 33) (see DISCUSSION). We collectively call these unmodeled effects "instantaneous stabilization" and, to investigate its effect on the observed adaptation performance, we have conducted the following additional analyses on the error clamp trials and EMG recordings, and *experiment 3*.

Adaptation Performance Is Determined Through an Interaction between Speed and Force Field Complexity

Taking together the results of two subexperiments done in *experiment 2*, the final statistical test tested if there is an interaction between the force field groups (N1 and N3) and speed conditions (FAST and SLOW) on the iAUC measures. A two-way mixed ANOVA with force field groups as a between-subject factor and speed as within-subject factor revealed that there was a significant and large interaction between experimental groups according to force complexities and speed conditions ($F_{1,14} = 16.663$, $P = 0.001$, the partial $\eta^2 = 0.543$, Greenhouse–Geisser corrected). This large interaction fits our hypothesis that the effect of encoding capacity is prominent only when the complexity of the force field is high, i.e., when the information to encode exceeds the encoding capacity.

Force Patterns during Error Clamp Trials Indicate the Evolution of Active Compensation Strategies

Our results can be further examined through the results of error clamp trials (Fig. 5). An error clamp trial was a single rotation randomly chosen among the middle of the twelve rotations per block, that is, between rotation 5 and 9, during which the hand movement was constrained within a circular mechanical channel generated along the reference circle (see *Error Clamp Trials* in MATERIALS AND METHODS). The amount of active compensation can be estimated by the pattern of the force that the participants applied to the mechanical channel. As the shape is the key factor that separates the N1 and N3 force fields, we first focus on how much the shape of the force field was learned.

For all four conditions, participants were able to learn active compensation: during the late-exposure phase (Fig. 5, blocks 35–47) Both N1-FAST and N1-SLOW showed single-peaked force compensation patterns, and N3-FAST and N3-SLOW showed triple-peaked compensation patterns. This suggests that the observed learnings were mainly based on an active, predictive compensation of the force field. However, while there was no noticeable difference between the compensation patterns of N1-FAST and N1-SLOW (Fig. 5, *A* and *B*), the shape of the compensation pattern of N3-FAST (Fig. 5*C*) was closer to the shape of the N3 force field compared to N3-SLOW (Fig. 5*D*), showing clearer and more distinct peaks. This supports our observations made on the normal trials that the learning performance was not significantly different between N1-FAST and N1-SLOW, but it was better in N3-FAST compared to N3-SLOW. The aftereffect were not particularly notable at either speed (Fig. 5, *C* and *D*, block 48).

Although the observed force compensation patterns in channel trials suggest that different speed conditions result in noticeable differences in the performance of compensating the force field imposed for non-channel trials, finding a single metric that can effectively summarize the above-mentioned trends of force compensation patterns poses a challenge. We adopted a matching-based metric for force compensation (25, 26) to quantify how much the forces were compensated (for definition, see MATERIALS AND METHODS). Figure 5*E* shows the resultant force compensation patterns. Once the force field was introduced, both N1 and N3 conditions showed an immediate increase in the force compensation level up to around 50%–60% within three blocks (~30 cycles). The initial force compensation levels of two speed conditions were not significantly different (Fig. 5*E*, blocks 10–12; $F_{1,7} = 0.030$; $P = 0.866$ for N1, $F_{1,7} = 1.637$; $P = 0.241$ for N3). However, different trends of the N1 and N3 groups were observed later in adaptation trials: The N1 group showed no significant increase in force compensation level for both speed conditions (Fig. 5*E*, *left*, blocks 10–11 and 45–47; $F_{4,28} = 0.504$; $P = 0.733$ for FAST and $F_{4,28} = 0.672$; $P = 0.617$ for SLOW), but the N3 group showed significant increases in force compensation level for the both speed conditions (Fig. 5*E*, *right*, blocks 10–11 and 45–47; $F_{4,28} = 3.355$; $P = 0.023$ for FAST and $F_{4,28} = 4.087$; $P = 0.010$ for SLOW). At the end of the training phase, the N3 group showed a significant difference in force compensation level between two speeds (Fig. 5*E*, *right*, blocks 45–47; $F_{1,7} = 10.306$; $P = 0.015$), but not in the N1 group (Fig. 5*E*, *left*, blocks 45–47; $F_{1,7} = 0.450$; $P = 0.524$). There were remarkable aftereffect compared to the preexposure phase for the SLOW condition in the N1 case (Fig. 5*E*, *left*, blocks 5–7 and 48; $F_{3,21} = 2.618$; $P = 0.078$ for the FAST and $F_{3,21} = 7.361$; $P = 0.001$ for the SLOW condition) and for both speed conditions in the N3 case (Fig. 5*E*, *right*, blocks 5–7 and 48; $F_{3,21} = 12.874$; $P < 0.001$ for the FAST and $F_{3,21} = 26.223$; $P < 0.001$ for the SLOW condition). Finally, the difference of the post-exposure phase force compensation between two speed conditions was not significant in the N1 case (Fig. 5*E*, *left*, block 48; $F_{1,7} = 1.320$; $P = 0.396$), but significant in the N3 case (Fig. 5*E*, *right*, block 48; $F_{1,7} = 5.732$; $P = 0.048$).

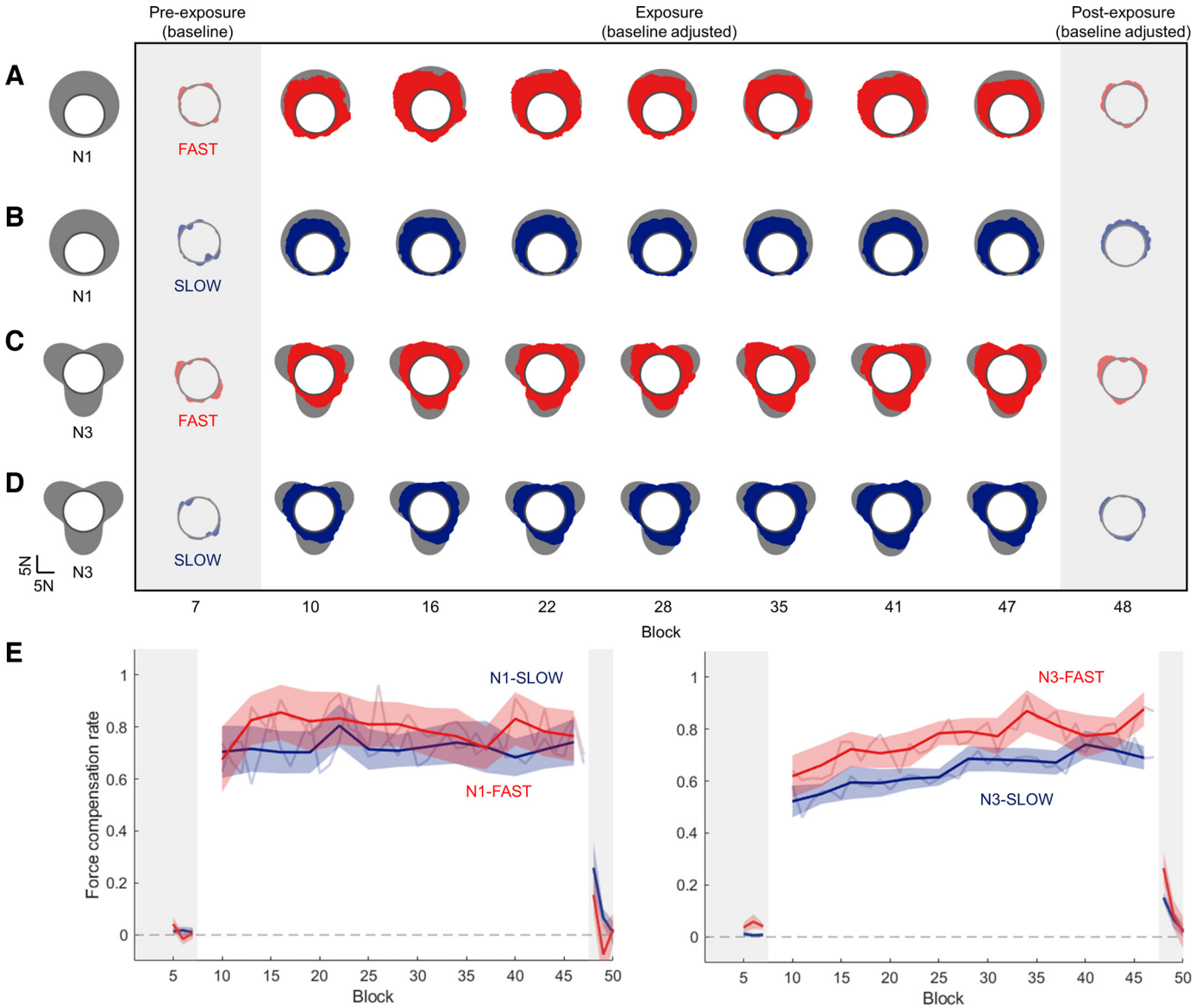

Figure 5. Force patterns during error clamp trials indicate the evolution of active compensation strategies. *A–D*: timelines of force profiles that participants applied against the mechanical channel during error clamp trials in different blocks, averaged over all eight participants per condition. Force profiles of the exposure and postexposure phases are baseline-adjusted by subtracting the average force profiles during the preexposure phase. The colored area is the trajectory of the force applied against the channel during error clamp trials in the N1-FAST (*A*), N1-SLOW (*B*), N3-FAST (*C*), and N3-SLOW (*D*) conditions, respectively, using the same color-coding used in the previous figures (i.e., red means FAST and blue means SLOW). The gray area behind the colored area represents the shape of the force field (N1 or N3) generated during normal exposure trials for each condition. For the participants experiencing flipped N1 or N3 force fields, force trajectories were also flipped and averaged together with participants experiencing nonflipped force fields. *E*: corresponding force compensation profiles of N1 (*left*) and N3 (*right*) groups. Force compensation curves are shown as the means ± standard error across three consecutive blocks of all eight participants ($n = 8$). The pale-colored graph of the background shows the magnitude of the force compensations on a per-block basis. One-way repeated-measures ANOVA was used for statistical tests on force compensation values.

The Benefit of Higher Speed Movement Does Not Originate from Increased Muscle Activities during Adaptation

To test how much the result of the N3 group, which showed a benefit of higher speed movement, was affected by increased muscle activities, we compared the EMG signals measured in N3-FAST and N3-SLOW. Figure 6 summarizes the change of EMG-levels for all four muscles, both for normal and channel trials. In overall, the EMG profiles show typical patterns of adaptation: higher EMG levels in the early-exposure phase followed by a gradual decrease throughout the exposure. For normal trials, two-way ANOVAs with phase (pre-, early- and late-exposure) and speed as within-subject factors revealed that there were significant effects of phase in general on the EMG levels of all four muscles (Fig. 6; biceps: $F_{2,10} = 22.071$, $P < 0.001$; Triceps: $F_{2,10} = 3.833$, $P = 0.058$; pectoralis: $F_{2,8} = 5.729$, $P = 0.029$; deltoid: $F_{2,10} = 9.098$, $P = 0.006$), but no significant main effect of speed was found for all four muscles (biceps: $F_{1,5} = 0.014$, $P = 0.912$; triceps: $F_{1,5} = 0.858$, $P = 0.397$; pectoralis: $F_{1,4} = 3.943$, $P = 0.118$; deltoid: $F_{1,5} = 0.228$, $P = 0.653$). In addition, no significant interaction between speed

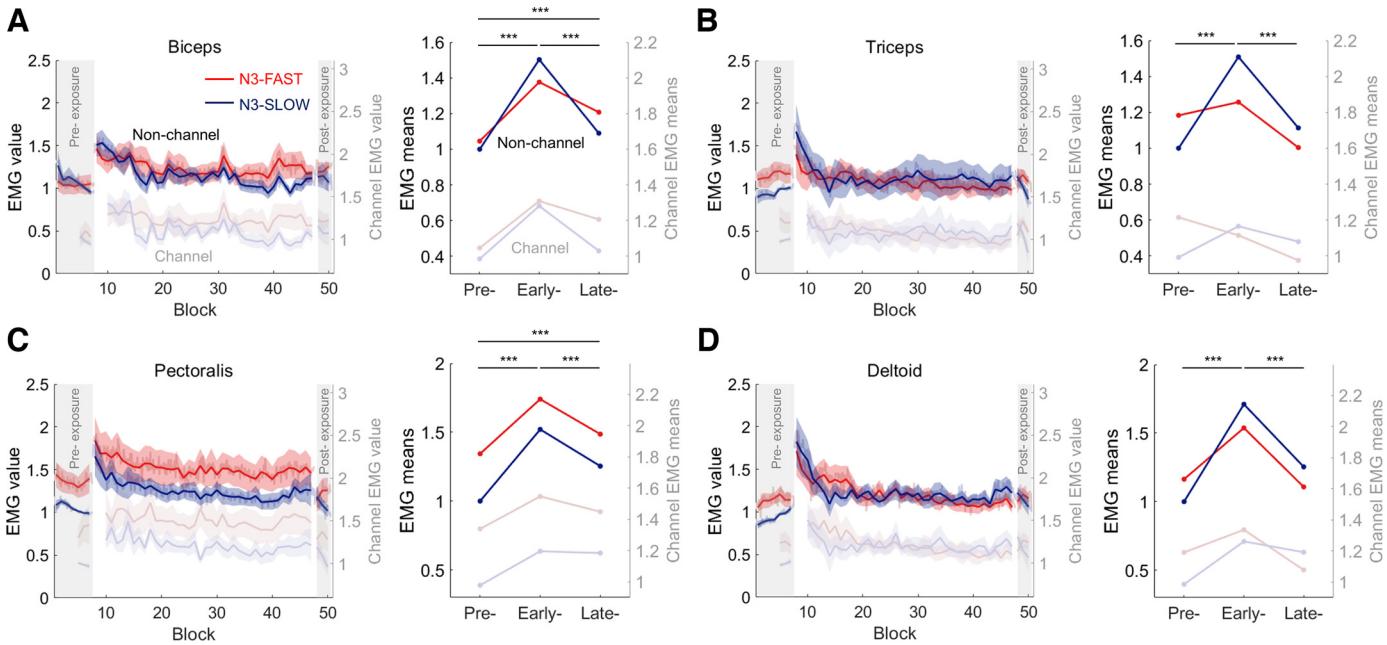

Figure 6. The benefit of higher speed movement does not originate from increased muscle activities during adaptation. Plots for normalized average EMG values for biceps (*A*), triceps (*B*), pectoralis (*C*), and deltoid (*D*) muscles in the N3-FAST (red) and N3-SLOW (blue) conditions for nonchannel and channel (offset below) trials. Before averaging, each EMG level for each participant was normalized with respect to the baseline EMG levels of the N3-SLOW condition (i.e., EMG values on blocks 5–7). For each muscle, the left subfigure shows the timelines of EMG levels during the N3-FAST (red) and N3-SLOW (blue) conditions, shown as block number vs. corresponding means ± standard error of participants ($n = 5$ for pectoralis and $n = 6$ for others). Overlapped with the block-averaged errors in thick colors, pale-colored plots in finer scales show the errors averaged per each cycle (one block contains 12 cycles). Offset below them, pale-colored plots show the EMG levels during channel trials. The right subfigure shows an interaction plot for EMG values between the three phases (blocks 5–7 for preexposure, blocks 8–10 for early-exposure, and blocks 45–47 for late-exposure) and the two speed conditions (FAST and SLOW). Offset below them, the pale-colored plot shows an interaction plot for EMG values during channel trials between the phases and speed conditions. Two-way repeated-measures ANOVA was used for statistical tests on normalized average EMG values. ***$P < 0.001$.

and phase was found for all four muscles (biceps: $F_{2,10} = 2.468$, $P = 0.134$; triceps: $F_{2,10} = 2.514$, $P = 0.130$; pectoralis: $F_{2,8} = 1.326$, $P = 0.318$; deltoid: $F_{2,10} = 1.920$, $P = 0.197$). The same results, that is, significant effects of phase, no significant effect of speed, and no significant interaction between phase and speed, were observed for channel trials (statistical test results omitted for simplicity). Altogether, the presented EMG analyses suggest that the observed differences in EMG levels between the SLOW and the FAST condition during adaptation were no different than those of the baseline. This indicates the observed advantage of the speed in adapting to the N3 force field is unlikely to result from muscle activations being particularly higher during adaptation. The similar trend observed on the EMG levels in channel trials also suggests that the levels of co-contraction were not particularly higher during N3-FAST adaptation and the baseline differences were maintained throughout the adaptation.

In addition to the block-averaged EMG levels, additional analysis was focused on the per-cycle EMG pattern to see if there was any noticeable change in the way muscles were activated during the circle drawing in different phases of the experiment. As within-cycle EMG patterns are highly variable across participants, the analysis was focused on data from representative participants. Figure 7 plots the average per-cycle EMG patterns for all four muscles of a single subject during five different phases of the experiment. First, the within-cycle EMG profiles in different adaptation phases well reflect the adaptation pattern observed in Fig. 6, showing an abrupt increase in EMG level in early exposure (blocks 7–8) followed by a gradual reduction throughout the exposure trials (blocks 8–47). While such reductions can be clearly seen in the FAST condition, only small amounts of reduction were observed in the SLOW condition for all four muscles, which confirms our observation in Fig. 6. Understanding the shapes of EMG profiles is not straightforward without additional analyses incorporating motion capture and inverse dynamics, which are out of the scope of our study. However, it can be observed that in the SLOW condition there are noticeable differences between the EMG patterns in the pre-exposure phase (block 7) and those in the end of adaptation (block 47), in terms of overall level and shape. This is in sharp contrast to the FAST condition where participants were able to restore to some extent the pre-exposure EMG patterns at the end of adaptation, except some fine modulations of timings (biceps) or activation levels (pectoralis). Note that the similarities between the EMG profiles of FAST and SLOW conditions at the end of adaptation (block 47) could be purely a coincidence since, as noted in the MATERIALS AND METHODS, force fields that each participant experienced in the FAST and SLOW conditions were flipped to each other. Although follow-up studies are required to confirm these observations, this may indicate that participants were able to come up with fine-tuned muscle activation patterns that efficiently compensate for the force field in the N3-FAST condition, while they were only able to compensate the force field with substantially higher and disparate muscle tones in the N3-SLOW condition.

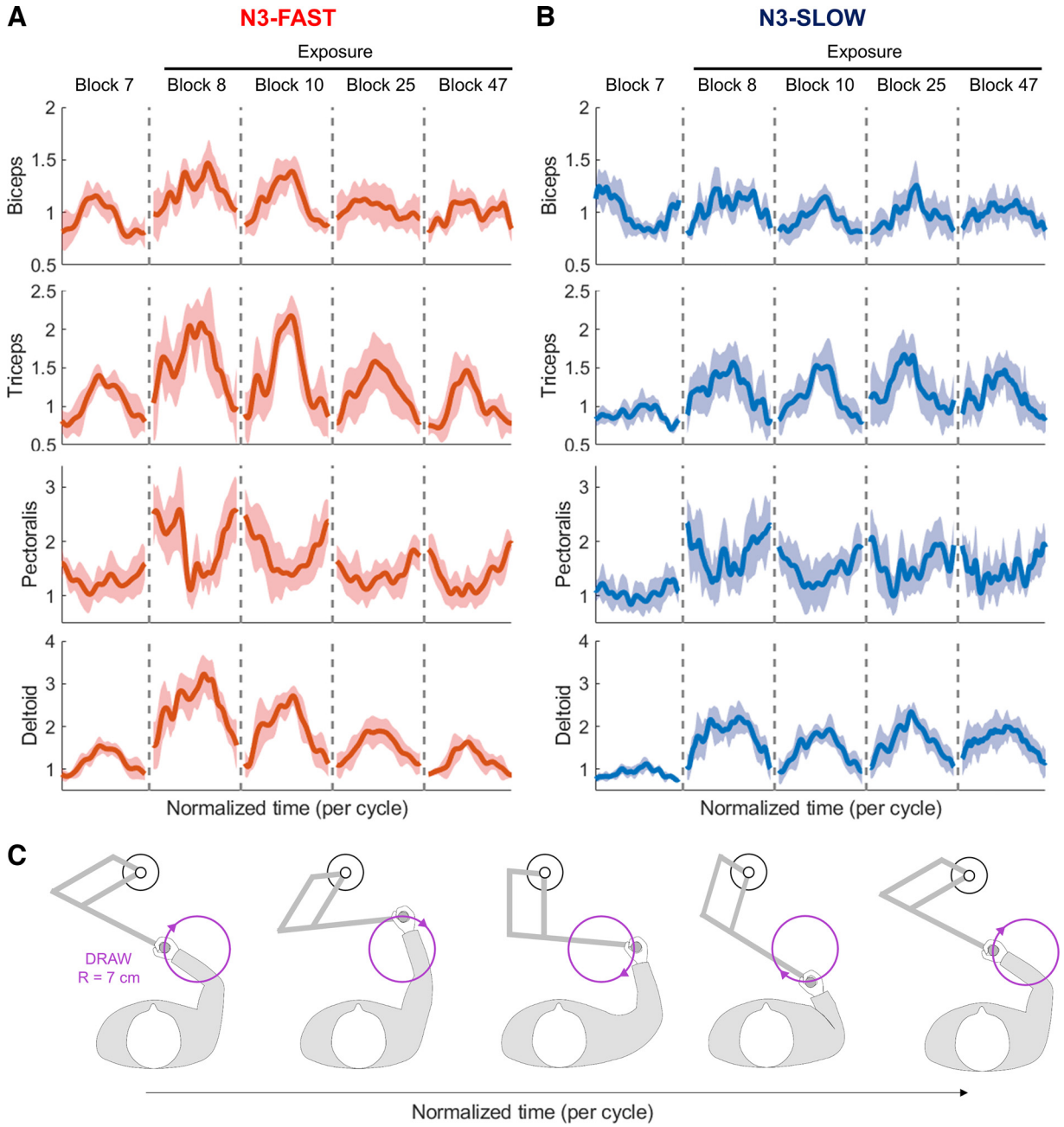

Figure 7. Within-cycle normalized EMG profile for N3-group of *experiment 2*. *A* and *B*: within-cycle normalized EMG profile for biceps, triceps, pectoralis, and deltoid muscles in the N3-FAST (*A*, red) and N3-SLOW (*B*, blue) conditions. For each muscle, the figure shows EMG profiles of a representative subject on the following three phases: preexposure (block 7), early-exposure (block 8), middle-exposure (blocks 10 and 25), and late-exposure (block 47). The EMG time series in each block (containing 12 cycles) is divided by individual cycles (i.e., drawing one circle), and in each cycle, the duration of the EMG profile is normalized. The EMG profiles of each muscle and each phase are shown as normalized time vs. corresponding means ± standard deviation across the cycles. *C*: illustration of arm configurations in five different time points within a cycle.

Experiment 3: The Benefit of Higher Speed Movement Is Related to the State-Dependent Policy

Experiment 3 was targeted to quantify the contribution of instantaneous stabilization to the observed benefit of fast movement in learning complex force field. Our hypothesis predicts that the adaptation performance would be significantly worse when learning the N3a force field since there is no state-dependent representation available. Alternatively, if the observed benefit of the fast movement is mainly from the instantaneous stabilization, there will be no performance difference between the two conditions.

Figure 8 summarizes the result of *experiment 3*. Comparing the average trajectories and adaptation curves for two conditions (Fig. 8, *C* and *D*), the initial error levels at the preexposure phase (Fig. 8*D*, blocks 5–7; $F_{1,7} = 0.189$, $P = 0.677$), the early-exposure phase before the instantaneous stabilization (Fig. 8*D*, block 8; $F_{1,7} = 1.832$, $P = 0.218$), and after the

J Neurophysiol • doi:10.1152/jn.00593.2020 • www.jn.org

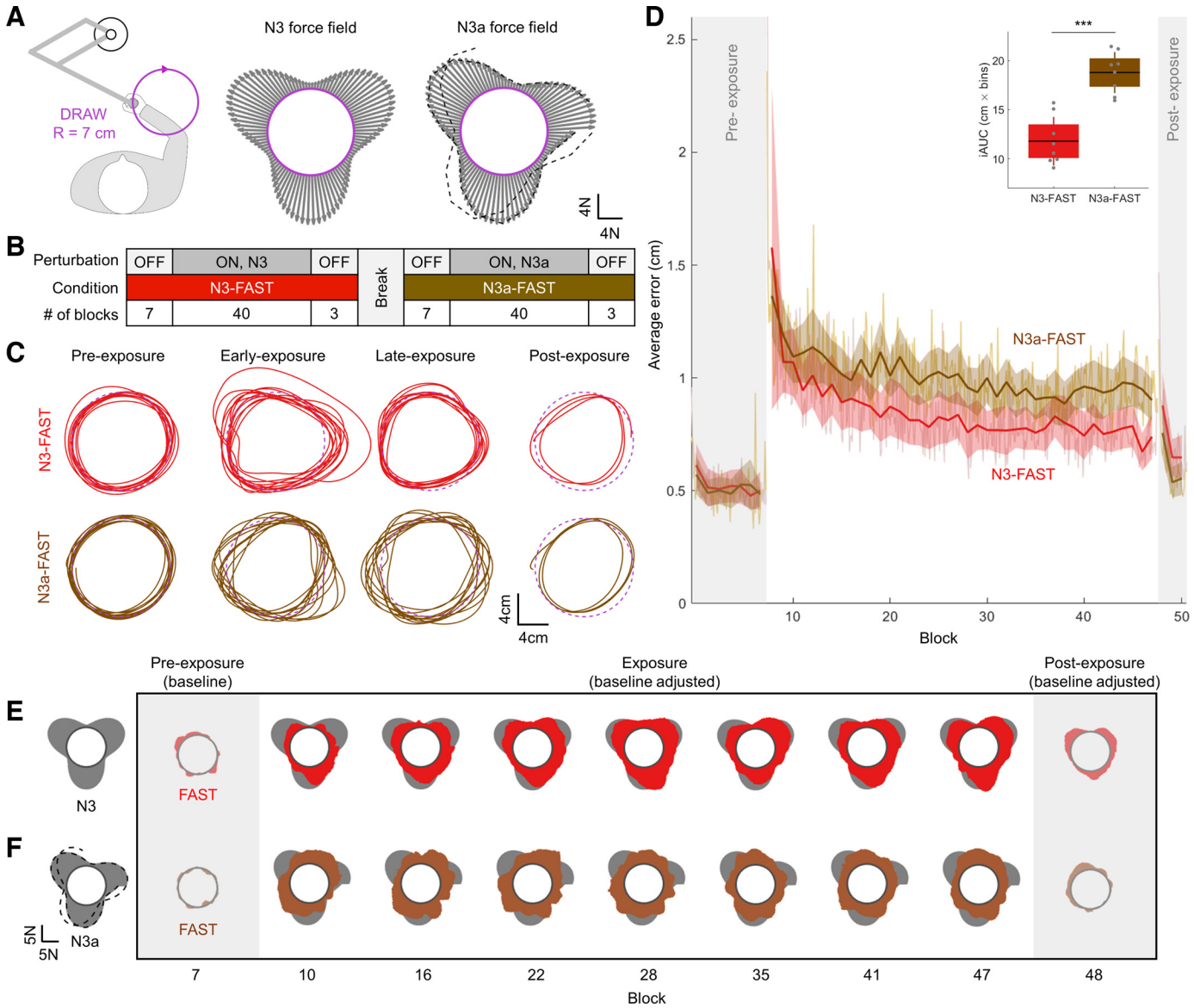

Figure 8. *Experiment 3*: the benefit of higher speed movement is related to the state-dependent policy. *A*: experimental setup. Subfigure on the right is a schematic diagram showing how the N3a force field is desynchronized. *B*: experimental protocol. *C*: representative hand paths of N3-FAST (red) and N3a-FAST (brown) during the preexposure (block 7), the early-exposure (block 8), the late-exposure (block 47), and the postexposure (block 48) phases. *D*: adaptation curves of the N3-FAST (red) and N3a-FAST (brown), shown as block number vs. corresponding means ± standard error of all eight participants ($n = 8$). The pale-colored graph in the background shows the magnitude of the errors on a per-cycle basis. One-way repeated-measures ANOVA was used for statistical tests on average errors. *Inset* is a box plot of iAUC values for each condition. A paired *t* test was used for statistical tests on iAUC values. Timelines of baseline-adjusted force profiles during error clamp trials in different blocks, averaged over all participants for the N3-FAST (*E*) and N3a-FAST (*F*). The gray area behind the colored area indicates the shape of the force field (N3 or N3a) generated during non-error clamp trials. ***$P < 0.001$. iAUC, incremental area under the curve.

instantaneous stabilization (Fig. 8*D*, block 10; $F_{1,7} = 0.110$, $P = 0.750$) and the patterns of quick reduction in the early-exposure phase was similar (Fig. 8*D*, blocks 9–10 and 45–47; $F_{4,28} = 28.776$, $P < 0.001$ for N3-FAST and $F_{4,28} = 9.728$, $P < 0.001$ for N3a-FAST), but it is clear that the gradual reduction of the error was not so prominent in N3a-FAST compare to N3-FAST (Fig. 8*D*, blocks 45–47; $F_{1,7} = 22.500$, $P = 0.002$), resulting in substantially higher iAUC in N3a-FAST during the exposure phase (Fig. 8*D*; $t_7 = -7.490$, $P < 0.001$). Looking at the aftereffect in the post-exposure phase, trajectories of N3-FAST and N3a-FAST showed inward distortions, but larger distortions, and therefore significantly higher aftereffect, were observed in N3-FAST. The aftereffect of N3-FAST with respect to the error level was significantly higher than that of N3a-FAST (Fig. 8*D*, block 48; $F_{1,7} = 5.775$; $P = 0.047$). Force patterns in the error clamp trials shown in Fig. 8, *E* and *F*, where the force pattern of the N3a-FAST was adjusted so that the perfect compensation would exactly match the underlying grey reference shape. The clear absence of peaks in N3a-FAST (Fig. 8*F*) compared to N3-FAST (Fig. 8*E*) suggests that participants could not develop any active strategy for compensation under the N3a force field. Taken together, these results support our hypothesis that the main benefit of the fast movement, observed during the entire course of

the adaptation, originates from the state-dependent adaptive mechanism that is specific to the shape of the force, whereas the effect of instantaneous stabilization mainly limited to early adaptation phase.

DISCUSSION

In this study, we have examined the effect of the encoding capacity of human motor adaptation, which describes how much information on newly experienced dynamics can be held by motor primitives. Our main hypothesis was that the performance of motor adaptation is upper limited by the encoding capacity that is determined by the size of the movement. In order to verify that, we have presented the results of three experiments which concluded, in brief, that *1*) learning requires movement, *2*) larger encoding space, that is, a higher speed movement, benefits learning complex dynamics, and *3*) such benefit of high-speed movement is a genuine aspect of motor learning, whereas the effect of instantaneous stabilization is limited only to the early phase.

In motor learning studies, the term "encoding" collectively refers to the process of internally representing sensorimotor information, such as body kinematics (12, 13, 16, 34, 35), action (11, 36–39), or perceived errors (10, 15, 40–42). In this study, encoding refers to the process of representing external dynamics (43–45). With this view, a key assumption of our study was that the encoding capacity is determined by the size of the state-space covered by the movement, which was also based on the predominant models of primitive-based motor learning (7, 9). Although this study combined existing terms and models widely used in the field, we proposed a novel perspective explaining how this primitive-based encoding procedure affects the performance of motor adaptation. As far as we know, this study is the first to experimentally show that such a limiting factor does exist in human motor adaptation and plays an important role in determining the adaptation performance.

To control the complexity of the dynamics to adapt, we introduced the concept of a complexity index. The complexity index is not exactly the same but was mentioned in previous papers under the name spatial frequency (7, 46). In the language of our paper, a higher spatial frequency of the force field contains a larger amount of information to be encoded and thus requires a larger encoding capacity. Our experimental designs were focused on examining the circumstances under which the encoding capacity was just above or below the amount of information of a complex force field and therefore significantly affects the adaptation performance, while the performance of learning a simpler force field is unaffected. The complexity indices used in the experiment, N1 and N3, along with different movement velocities, FAST and SLOW, successfully captured the interaction between the complexity of the external dynamics and the encoding capacity.

In our study, the encoding capacity was modulated by changing the movement speed. An alternative, or even a more intuitive choice would have been to change the positional properties, for example, the radius of the reference circle. However, we decided to keep the positional properties constant in order to avoid comparing the performance of movements in different arm configurations. For this reason, we focused on assessing the effect of different speeds in motor adaptation performance while keeping the shape of the trajectory constant. Although this design was necessary for the fair comparison, it posed some significant but unavoidable challenges: The most obvious source of complication was the effect of the signal-dependent noise. Not surprisingly, movement with a different speed causes a default difference in the baseline performances and also in the initial error levels of the adaptation phase, which makes it hard to definitely determine whether the learning performance in one condition is better than the other, even with the widely-used iAUC-based comparison incorporated in our study. In addition, since the number of trials was fixed, different movement speeds resulted in different durations of the adaptation. Because of these complicated factors, our analysis was mainly focused on highlighting how the effect of movement speed interacts with force field complexities. The clear interaction shown in our result suggests that, if and only if the complexity of the force field exceeds the encoding capacity, the adaptation performance becomes bottlenecked.

Our result shows the benefit of high-speed movement in learning new external dynamics. Such effect of movement speed in motor adaptation has not been studied previously, but there exist studies on speed generalization, investigating how a motor skill acquired in one speed generalizes to different speeds (13, 47–49). Specifically, studies have suggested that the extrapolation quality of the speed along a single movement direction, that is, how learning generalizes when movement is made in the same direction but with a speed outside of the training range, is substantially better compared to what is predicted by the Gaussian-like primitives, implying that generalization of learning in velocity space may not be local, and the shape of the primitives in position-velocity space could be anisotropic (13, 48). Our study deliberately avoided this potential complication by incorporating circular movements, in which the direction of the velocity varies constantly.

Similar to other motor learning studies, it is possible that the observed adaptation behaviors are affected by certain cognitive strategies. However, our experimental design effectively rules out such possibilities. First of all, the result of *experiment 1* strongly suggests that participants are not able to utilize any cognitive strategy in our adaptation tasks. In the HOLD condition in *experiment 1*, participants were asked to hold the handle still against the repeated pattern of force perturbations. Our result clearly shows that, even though participants had sufficient understanding on how the direction and magnitude of the force perturbation were repeated, none of them were able to effectively compensate for such perturbation. Although this confirms our main hypothesis that zero encoding capacity renders zero learning, this also suggests that, in more complex adaptation scenarios in *experiment 2* and *experiment 3*, the chance that any cognitive strategy was developed and involved during adaptation is very limited. Second, even if we assume that some explicit strategies were involved in the earlier phase of the adaptation, it is highly likely that such strategies might have been overridden by an implicit strategy after prolonged training (50). Last, even when participants were able to keep using cognitive strategies in the SLOW condition throughout the entire training, making persistent efforts to keep such

strategies does not seem to be a successful choice from the performance perspective, because the observed performances in SLOW condition were no more effective than that of the FAST condition for the N1 group, and significantly less effective than the FAST condition for the N3 group. All these results strongly suggest that the effect of cognitive strategy on our result is minimal.

Although the observed adaptation patterns are largely consistent with the conventional pattern of motor adaptation, we also observed a different type of benefit of fast movement, called instantaneous stabilization, that is effective in the early stages of adaptation and de-adaptation. It is possible that such stabilization effect simply originates from the increased impedance of upper limb in high-speed movements, which is known to play the main role in stabilizing movement in the early phase of force field adaptation (51, 52) and also known to be able to compensate specific pattern of instability (53, 54), including the uncertainty induced by signal-dependent noise (55, 56). However, our EMG analysis suggested that this stabilization effect may not be caused solely by the impedance mechanism since, unlike previous studies where higher levels of EMG signals were reported (51, 52, 57), differences in muscle activation levels between FAST and SLOW condition during adaptation were no greater than their baseline differences. It is possible that the instantaneous stabilization effect may originate from the ability of our brain that quickly develops a crude estimation of the perturbing forces and corresponding feedforward mechanism, as early as the second exposure to the force field (58). It is important to note that our circle-drawing experiments involve longer trials (twelve continuous cycles) compared to the conventional point-to-point reaching experiments. For this reason, it is possible that the participants already developed a crude internal model that roughly compensates the external force field during the first block of the exposure phase. In any case, we have shown that this instantaneous stabilization does not undermine the main conclusion of the paper. Our follow-up experiment (*experiment 3*) has confirmed that the effect of instantaneous stabilization is only limited to the early phase of the adaptation.

We also incorporate the error clamp trials using mechanical channels to better assess the feedforward component of the adaptation. Although error clamp trials in previous studies were used for point-to-point movements (24), our study is the first, as far as we are aware, to implement a circular version of the error clamp trial. Compared with the point-to-point movements where each movement is distinct from the other, and also the target direction and the error are always constant, we have encountered several technical issues in implementing error clamp trials for continuous circular movements, and have come up with novel technical solutions. For example, we made the force channel to be gradually engaged and disengaged in order to prevent noticeable mechanical impacts when entering the channel, where the details can be found in "*Error Clamp Trials*" of MATERIAL AND METHODS. Despite these solutions, it was still challenging to make a circular error clamp trial that feels perfectly the same as the conventional error clamp trials, and it is possible that this different force feedback that participants experienced during error clamp trials may have induced a contextual effect (59, 60) separating the motor memories of normal and error clamp trials. In addition to the effect of instantaneous stabilization, this contextual effect could have potentially contributed to the observed force compensation patterns that look somewhat different from the conventional patterns. However, it can be clearly seen from the recorded force patterns in error clamp trials shown in Fig. 5, which closely resembles the force field patterns in the late adaptation phase, that our error clamp trials can successfully capture the aspect of learning.

Taken together, we have experimentally shown that the effect of encoding capacity works as a major limiting factor of the performance of motor adaptation. Our result highlighted the importance of securing a large encoding space, i.e., making larger movements, in order to learn complex dynamics of the body and environment.

ACKNOWLEDGMENTS

The authors thank Yujing Zhang for participating in the data collection of the study.

GRANTS

This work was financially supported by the Institute for Information & Communication Technology Promotion (No. 2019-0-01367, BabyMind, https://babymind-project.github.io/) to S.-H.Y and F.C.P., the National Research Foundation of Korea (NRF-2016R1A5A1938472, http://www.src-erc.or.kr/) to F.C.P., the Biomimetic Robot Research Center (DAPAUD190018ID) to F.C.P., the BK21 plus program (https://bkplus.nrf.re.kr/) to F.C.P., the Artificial Intelligence Institute of Seoul National University (https://aiis.snu.ac.kr/) to F.C.P., the Institute of Advanced Machines and Design (http://iamd.snu.ac.kr/) to F.C.P., and Biotechnology and Biological Sciences Research Council (BB/S003762/1) to S.-H.Y.

DISCLOSURES

No conflicts of interest, financial or otherwise, are declared by the authors.

AUTHOR CONTRIBUTIONS

S.K., J.K. and S.-H.Y. conceived and designed research; S.K., J.K., and J.-M.K. performed experiments; S.K., J.K., J.-M.K., and S.-H.Y. analyzed data; S.K., J.K., J.-M.K., and S.-H.Y. interpreted results of experiments; S.K. prepared figures; S.K. drafted manuscript; S.K., J.K., F.C.P., and S.-H.Y. edited and revised manuscript; F.C.P. and S.-H.Y. approved final version of manuscript.

REFERENCES

1. **Harris CM**, **Wolpert DM.** Signal-dependent noise determines motor planning. *Nature* 394: 780–784, 1998. doi:10.1038/29528.
2. **Hollerbach MJ**, **Flash T.** Dynamic interactions between limb segments during planar arm movement. *Biol Cybern* 44: 67–77, 1982. doi:10.1007/BF00353957.
3. **Alexander RM.** A minimum energy cost hypothesis for human arm trajectories. *Biol Cybern* 76: 97–105, 1997. doi:10.1007/s004220050324.
4. **Diedrichsen J**, **Shadmehr R**, **Ivry RB.** The coordination of movement: optimal feedback control and beyond. *Trends Cogn Sci* 14: 31–39, 2010. doi:10.1016/j.tics.2009.11.004.
5. **Scott SH.** The computational and neural basis of voluntary motor control and planning. *Trends Cogn Sci* 16: 541–549, 2012. doi:10.1016/j.tics.2012.09.008.

6. **Todorov E**, **Jordan MI.** Optimal feedback control as a theory of motor coordination. *Nat Neurosci* 5: 1226–1235, 2002. doi:10.1038/nn963.
7. **Thoroughman KA**, **Shadmehr R.** Learning of action through adaptive combination of motor primitives. *Nature* 407: 742–747, 2000. doi:10.1038/35037588.
8. **Wolpert DM**, **Diedrichsen J**, **Flanagan JR.** Principles of sensorimotor learning. *Nat Rev Neurosci* 12: 739–751, 2011. doi:10.1038/nrn3112.
9. **Castro LNG**, **Monsen CB**, **Smith MA.** The binding of learning to action in motor adaptation. *PLoS Comput Biol* 7: e1002052, 2011. doi:10.1371/journal.pcbi.1002052.
10. **Herzfeld DJ**, **Vaswani PA**, **Marko MK**, **Shadmehr R.** A memory of errors in sensorimotor learning. *Science* 345: 1349–1353, 2014. doi:10.1126/science.1253138.
11. **Howard IS**, **Ingram JN**, **Franklin DW**, **Wolpert DM.** Gone in 0.6 seconds: the encoding of motor memories depends on recent sensorimotor states. *J Neurosci* 32: 12756–12768, 2012. doi:10.1523/JNEUROSCI.5909-11.2012.
12. **Hwang EJ**, **Donchin O**, **Smith MA**, **Shadmehr R.** A gain-field encoding of limb position and velocity in the internal model of arm dynamics. *PLoS Biol* 1: e25, 2003. doi:10.1371/journal.pbio.0000025.
13. **Joiner WM**, **Ajayi O**, **Sing GC**, **Smith MA.** Linear hypergeneralization of learned dynamics across movement speeds reveals anisotropic, gain-encoding primitives for motor adaptation. *J Neurophysiol* 105: 45–59, 2011. doi:10.1152/jn.00884.2009.
14. **Sing GC**, **Joiner WM**, **Nanayakkara T**, **Brayanov JB**, **Smith MA.** Primitives for motor adaptation reflect correlated neural tuning to position and velocity. *Neuron* 64: 575–589, 2009. doi:10.1016/j.neuron.2009.10.001.
15. **Takiyama K**, **Hirashima M**, **Nozaki D.** Prospective errors determine motor learning. *Nat Commun* 6: 5925, 2015. doi:10.1038/ncomms6925.
16. **Donchin O**, **Francis JT**, **Shadmehr R.** Quantifying generalization from trial-by-trial behavior of adaptive systems that learn with basis functions: theory and experiments in human motor control. *J Neurosci* 23: 9032–9045, 2003. doi:10.1523/JNEUROSCI.23-27-09032.2003.
17. **Donchin O**, **Shadmehr R.** Linking motor learning to function approximation: learning in an unlearnable force field. In: *Advances in Neural Information Processing Systems* 14, edited by Dietterich TG, Becker S, Ghahramani Z. Cambridge, MA: MIT Press, 2002, p. 197–203.
18. **Jones KE**, **Hamilton AF**, **Wolpert DM.** Sources of signal-dependent noise during isometric force production. *J Neurophysiol* 88: 1533–1544, 2002. doi:10.1152/jn.2002.88.3.1533.
19. **Therrien AS**, **Wolpert DM**, **Bastian AJ.** Increasing motor noise impairs reinforcement learning in healthy individuals. *eNeuro* 5: ENEURO.0050-18.2018, 2018. doi:10.1523/ENEURO.0050-18.2018.
20. **Oldfield RC.** The assessment and analysis of handedness: the Edinburgh inventory. *Neuropsychologia* 9: 97–113, 1971. doi:10.1016/0028-3932(71)90067-4.
21. **Howard IS**, **Ingram JN**, **Wolpert DM.** A modular planar robotic manipulandum with end-point torque control. *J Neurosci Methods* 181: 199–211, 2009. doi:10.1016/j.jneumeth.2009.05.005.
22. **Howard IS**, **Ingram JN**, **Wolpert DM.** Separate representations of dynamics in rhythmic and discrete movements: evidence from motor learning. *J Neurophysiol* 105: 1722–1731, 2011. doi:10.1152/jn.00780.2010.
23. **Weightman M**, **Brittain J-S**, **Punt D**, **Miall RC**, **Jenkinson N.** Targeted tDCS selectively improves motor adaptation with the proximal and distal upper limb. *Brain Stimul* 13: 707–716, 2020. doi:10.1016/j.brs.2020.02.013.
24. **Scheidt RA**, **Reinkensmeyer DJ**, **Conditt MA**, **Rymer WZ**, **Mussa-Ivaldi FA.** Persistence of motor adaptation during constrained, multijoint, arm movements. *J Neurophysiol* 84: 853–862, 2000. doi:10.1152/jn.2000.84.2.853.
25. **Reuter E-M**, **Cunnington R**, **Mattingley JB**, **Riek S**, **Carroll TJ.** Feedforward compensation for novel dynamics depends on force field orientation but is similar for the left and right arms. *J Neurophysiol* 116: 2260–2271, 2016. doi:10.1152/jn.00425.2016.
26. **Smith MA**, **Ghazizadeh A**, **Shadmehr R.** Interacting adaptive processes with different timescales underlie short-term motor learning. *PLoS Biol* 4: e179, 2006. doi:10.1371/journal.pbio.0040179.
27. **Conditt MA**, **Mussa-Ivaldi FA.** Central representation of time during motor learning. *Proc Natl Acad Sci USA* 96: 11625–11630, 1999. doi:10.1073/pnas.96.20.11625.
28. **Diedrichsen J**, **Criscimagna-Hemminger SE**, **Shadmehr R.** Dissociating timing and coordination as functions of the cerebellum. *J Neurosci* 27: 6291–6301, 2007. doi:10.1523/JNEUROSCI.0061-07.2007.
29. **Karniel A**, **Mussa-Ivaldi FA.** Sequence, time, or state representation: how does the motor control system adapt to variable environments? *Biol Cybern* 89: 10–21, 2003. doi:10.1007/s00422-003-0397-7.
30. **Franklin DW**, **Osu R**, **Burdet E**, **Kawato M**, **Milner TE.** Adaptation to stable and unstable dynamics achieved by combined impedance control and inverse dynamics model. *J Neurophysiol* 90: 3270–3282, 2003. doi:10.1152/jn.01112.2002.
31. **Gomi H**, **Osu R.** Task-dependent viscoelasticity of human multijoint arm and its spatial characteristics for interaction with environments. *J Neurosci* 18: 8965–8978, 1998. doi:10.1523/JNEUROSCI.18-21-08965.1998.
32. **Franklin S**, **Wolpert DM**, **Franklin DW.** Visuomotor feedback gains upregulate during the learning of novel dynamics. *J Neurophysiol* 108: 467–478, 2012. doi:10.1152/jn.01123.2011.
33. **Pruszynski JA**, **Kurtzer I**, **Scott SH.** Rapid motor responses are appropriately tuned to the metrics of a visuospatial task. *J Neurophysiol* 100: 224–238, 2008. doi:10.1152/jn.90262.2008.
34. **Hwang EJ**, **Smith MA**, **Shadmehr R.** Adaptation and generalization in acceleration-dependent force fields. *Exp Brain Res* 169: 496–506, 2006. doi:10.1007/s00221-005-0163-2.
35. **Hwang EJ**, **Shadmehr R.** Internal models of limb dynamics and the encoding of limb state. *J Neural Eng* 2: S266–S278, 2005. doi:10.1088/1741-2560/2/3/S09.
36. **Brayanov JB**, **Press DZ**, **Smith MA.** Motor memory is encoded as a gain-field combination of intrinsic and extrinsic action representations. *J Neurosci* 32: 14951–14965, 2012. doi:10.1523/JNEUROSCI.1928-12.2012.
37. **Gallivan JP**, **Bowman NAR**, **Chapman CS**, **Wolpert DM**, **Flanagan JR.** The sequential encoding of competing action goals involves dynamic restructuring of motor plans in working memory. *J Neurophysiol* 115: 3113–3122, 2016. doi:10.1152/jn.00951.2015.
38. **Gallivan JP**, **Stewart BM**, **Baugh LA**, **Wolpert DM**, **Flanagan JR.** Rapid automatic motor encoding of competing reach options. *Cell Rep* 19: 890–893, 2017. doi:10.1016/j.celrep.2017.04.034.
39. **Herzfeld DJ**, **Kojima Y**, **Soetedjo R**, **Shadmehr R.** Encoding of action by the Purkinje cells of the cerebellum. *Nature* 526: 439–442, 2015. doi:10.1038/nature15693.
40. **Fine MS**, **Thoroughman KA.** Trial-by-trial transformation of error into sensorimotor adaptation changes with environmental dynamics. *J Neurophysiol* 98: 1392–1404, 2007. doi:10.1152/jn.00196.2007.
41. **Schlerf J**, **Ivry RB**, **Diedrichsen J.** Encoding of sensory prediction errors in the human cerebellum. *J Neurosci* 32: 4913–4922, 2012. doi:10.1523/JNEUROSCI.4504-11.2012.
42. **Tseng Y-W**, **Diedrichsen J**, **Krakauer JW**, **Shadmehr R**, **Bastian AJ.** Sensory prediction errors drive cerebellum-dependent adaptation of reaching. *J Neurophysiol* 98: 54–62, 2007. doi:10.1152/jn.00266.2007.
43. **Berniker M**, **Franklin DW**, **Flanagan JR**, **Wolpert DM**, **Kording K.** Motor learning of novel dynamics is not represented in a single global coordinate system: evaluation of mixed coordinate representations and local learning. *J Neurophysiol* 111: 1165–1182, 2014. doi:10.1152/jn.00493.2013.
44. **Malfait N**, **Gribble PL**, **Ostry DJ.** Generalization of motor learning based on multiple field exposures and local adaptation. *J Neurophysiol* 93: 3327–3338, 2005. doi:10.1152/jn.00883.2004.
45. **Shadmehr R**, **Mussa-Ivaldi FA.** Adaptive representation of dynamics during learning of a motor task. *J Neurosci* 14: 3208–3224, 1994. doi:10.1523/JNEUROSCI.14-05-03208.1994.
46. **Thoroughman KA**, **Taylor JA.** Rapid reshaping of human motor generalization. *J Neurosci* 25: 8948–8953, 2005. doi:10.1523/JNEUROSCI.1771-05.2005.
47. **Francis JT.** Error generalization as a function of velocity and duration: human reaching movements. *Exp Brain Res* 186: 23–37, 2008. doi:10.1007/s00221-007-1202-y.
48. **Goodbody SJ**, **Wolpert DM.** Temporal and amplitude generalization in motor learning. *J Neurophysiol* 79: 1825–1838, 1998. doi:10.1152/jn.1998.79.4.1825.

49. **Mattar AAG**, **Ostry DJ.** Generalization of dynamics learning across changes in movement amplitude. *J Neurophysiol* 104: 426–438, 2010. doi:10.1152/jn.00886.2009.
50. **Mazzoni P**, **Krakauer JW.** An implicit plan overrides an explicit strategy during visuomotor adaptation. *J Neurosci* 26: 3642–3645, 2006. doi:10.1523/JNEUROSCI.5317-05.2006.
51. **Milner TE**, **Cloutier C.** Compensation for mechanically unstable loading in voluntary wrist movement. *Exp Brain Res* 94: 522–532, 1993. doi:10.1007/BF00230210.
52. **Osu R**, **Franklin DW**, **Kato H**, **Gomi H**, **Domen K**, **Yoshioka T**, **Kawato M.** Short- and long-term changes in joint co-contraction associated with motor learning as revealed from surface EMG. *J Neurophysiol* 88: 991–1004, 2002. doi:10.1152/jn.2002.88.2.991.
53. **Burdet E**, **Osu R**, **Franklin DW**, **Milner TE**, **Kawato M.** The central nervous system stabilizes unstable dynamics by learning optimal impedance. *Nature* 414: 446–449, 2001. doi:10.1038/35106566.
54. **Franklin DW**, **Liaw G**, **Milner TE**, **Osu R**, **Burdet E**, **Kawato M.** Endpoint stiffness of the arm is directionally tuned to instability in the environment. *J Neurosci* 27: 7705–7716, 2007. doi:10.1523/JNEUROSCI.0968-07.2007.
55. **Osu R**, **Kamimura N**, **Iwasaki H**, **Nakano E**, **Harris CM**, **Wada Y**, **Kawato M.** Optimal impedance control for task achievement in the presence of signal-dependent noise. *J Neurophysiol* 92: 1199–1215, 2004. doi:10.1152/jn.00519.2003.
56. **Selen LPJ**, **Franklin DW**, **Wolpert DM.** Impedance control reduces instability that arises from motor noise. *J Neurosci* 29: 12606–12616, 2009. doi:10.1523/JNEUROSCI.2826-09.2009.
57. **Thoroughman KA**, **Shadmehr R.** Electromyographic correlates of learning an internal model of reaching movements. *J Neurosci* 19: 8573–8588, 1999. doi:10.1523/JNEUROSCI.19-19-08573.1999.
58. **Milner TE**, **Franklin DW.** Impedance control and internal model use during the initial stage of adaptation to novel dynamics in humans. *J Physiol* 567: 651–664, 2005. doi:10.1113/jphysiol.2005.090449.
59. **Howard IS**, **Wolpert DM**, **Franklin DW.** The effect of contextual cues on the encoding of motor memories. *J Neurophysiol* 109: 2632–2644, 2013. doi:10.1152/jn.00773.2012.
60. **Wolpert DM**, **Flanagan JR.** Computations underlying sensorimotor learning. *Curr Opin Neurobiol* 37: 7–11, 2016. doi:10.1016/j.conb.2015.12.003.